Carbon nanodots-based nanocomposites with enhanced photocatalytic performance and photothermal effects

J. Zhang,[1,a)] Y. L. Tang,[1] G. Hu,[1] B. L. Gao,[1] Z. X. Gan,[3] and P. K. Chu[2,a)]
[1]*Faculty of Mathematics and Physics, Huaiyin Institute of Technology, Huaian 223003, China*
[2]*Department of Physics and Materials Science, City University of Hong Kong, Tat Chee Avenue, Kowloon, Hong Kong, China*
[3]*School of Physics and Technology, Nanjing Normal University, Nanjing 210023, China*

(Received 4 May 2017; accepted 24 June 2017; published online 6 July 2017)

Carbon nanomaterials with variable bandgaps exhibit wide spectral absorption, and photoluminescent nanodots have attracted much interest. In this work, carbon nanodots (CNDs) are grafted onto the surface of TiO_2 nanotubes to enhance the photocatalytic properties. The CNDs increase light absorption, trap and shuttle photo-generated electrons, and enhance the pollutant adsorptivity. In addition, the synergistic photothermal effect of the CNDs-based nanocomposite facilitates photocatalysis. The CNDs-based nanocomposites with improved photothermal performance and efficient photocatalytic characteristics have large potential in environment and energy applications. *Published by AIP Publishing.* [http://dx.doi.org/10.1063/1.4992132]

Owing to the distinctive morphology and vertically oriented nanostructure, TiO_2 nanotube arrays (TiNTs) have aroused scientific interests for the good performance in photocatalysis and photoelectrochemistry.[1,2] However, pure TiNTs have a wide bandgap which restricts optical energy conversion, and measures to maximize the utilization of solar energy have been proposed.[3–6]

Carbon nanodots (CNDs) have outstanding optical properties, dispersibility in water, excellent biocompatibility, and low toxicity.[7–9] Recently, researchers have exploited these attractive properties by preparing nanocomposites comprising CNDs.[10–15] The four common functions of CNDs are trapping of photo-generated electrons, extension of light absorption, enrichment of pollutants on composites,[16] and upconversion.[17,18] CNDs also exhibit photothermal effects, and Ge *et al.*[19] have reported red luminescent CNDs with a photothermal conversion efficiency of 38.5% when irradiated with the 671 nm laser. The strong photothermal effect is a key factor in the photocatalytic performance, but up to now it has not been studied in details. Herein, photo-degradation of methylene blue (MB) by the TiO_2-CNDs nanocomposite is investigated, and the role played by the photothermal effect in the degradation of organic pollutants is determined.

The TiNTs were fabricated by electrochemical anodization of titanium (Ti) foils (99.6% pure). The chemical reagents used in the experiments were of analytical grade and used without purification. After cleaning with acetone, ethanol, and deionized water, the Ti sheets were chemically etched by dipping into a solution containing NH_4F (0.5 wt. %), glycerol and water ($V_{glycerol}$:V_{water} = 17:3). Anodization was performed on a two-electrode electrochemical cell at a constant voltage of 50 V for 5 h.[20] After anodization, the samples were rinsed with deionized water, dried in air, and annealed at 450 °C for 2 h.

The CNDs were prepared by the modified Kang's method.[17] In short, graphite rods were used as the anode and cathode simultaneously, and the electrolyte was an ethanol/H_2O solution (volume ratio of 99.5:0.5) containing 0.5 g of NaOH. Since CNDs are produced with a small current density emitted light with longer wavelengths under irradiation,[14] electrochemical oxidation was carried out at a current intensity of 20 mA cm^{-2} for 10 h. After the reaction, a suitable amount of anhydrous $MgSO_4$ (5 wt. %) was added to the solution, stirred for 1 h, and stored for 24 h. The solid salts were then removed by centrifugation, and after ethanol was evaporated at a reduced pressure, the CND powders were obtained.

The TiNTs sheets were placed in a Teflon-sealed autoclave and immersed in CND solutions with different concentrations of 25, 50, and 75 μg/ml. The autoclave was placed in an oven at 120 °C for 10 h. For comparison, some TiNT sheets were processed under the same hydrothermal conditions without CNDs. The samples were washed with deionized water and dried at room temperature prior to the photocatalytic experiments. Degradation of these samples is presented in Fig. S1 in supplementary material. The samples prepared with the 50 μg/ml CND solution are the most efficient, and so, these CNDs/TiNTs were chosen to study the photothermal effect.

X-ray diffraction (XRD) was conducted on a X'PERT diffractometer (Philips Corporation, Holland), and X-ray photoelectron spectroscopy (XPS) was performed on a K-Alpha spectrometer (Thermo Fisher Scientific Corporation, USA). The microstructure and morphology of the samples were examined by scanning electron microscopy (SEM, Hitachi-3400N, Japan) and high-resolution transmission electron microscopy (HR-TEM, JEOL JEM-4000EX). The UV-Vis absorption spectra were acquired on a UV-Vis spectrophotometer (UV-2550, Shimadzu). The photoluminescence (PL) measurements were conducted on an Edinburgh FLS-920 PL spectrometer, and Raman scattering was performed on a T64000 triple Raman system.

The CNDs were nearly spherical in shape as shown in Fig. 1(a), and the particle diameter is about 5 nm. The inset

a)Authors to whom correspondence should be addressed: zhangjun@hyit.edu.cn and paul.chu@cityu.edu.hk

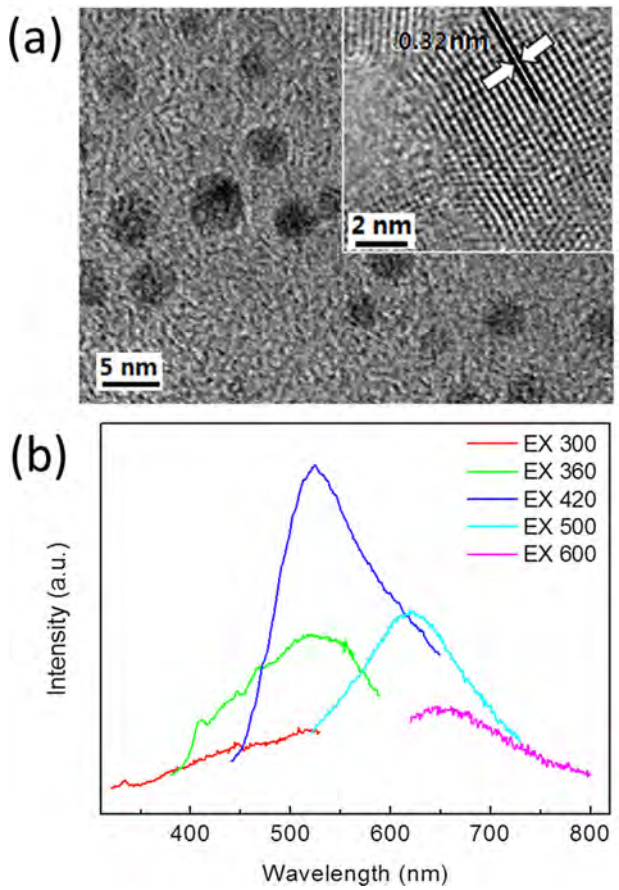

FIG. 1. (a) TEM image of CNDs with the inset showing the HR-TEM image of the typical CND. (b) Photoluminescence emission spectra (progressively longer excitation wavelengths from 300 nm to 600 nm) of the CNDs.

in Fig. 1(a) confirms the crystalline structure of the CNDs with an interplanar distance of 0.32 nm. It deviates slightly from the lattice spacing of the (002) plane of bulk carbon, i.e., 0.338 nm of JCPDS card No. 41-1487 and 0.329 nm of JCPDS card No. 46-0943. Nevertheless, when the structure is ultra-small (<10 nm), there are surface stress and strain at surface and an interplanar distance (002) of 0.32 nm has been observed from CNDs.[14,21] Figure 1(b) shows the PL spectra of the CNDs, and the emission spectra range from 400 to 800 nm according to the excitation. The PL quantum yield of the CNDs is determined to be 0.7%, and the low value may be attributed to the efficient non-radiative pathways and vibrational relaxation enabled by the high frequency core and surface modes.[22]

The morphology of the TiNTs is shown in Fig. 2. Similar to that observed previously,[20] the TiNTs have a mean inner diameter of about 200 nm, and the nanotubes are up to 3 μm in length (inset). After decoration with CNDs, the tubes maintain the geometry with the CNDs attached to the nanotubes, and some CNDs gather on the top of the tubes as shown in Fig. 2(b). Figure 2(c) displays the magnified HR-TEM image (inset) showing the presence of CNDs on the tubes. As a result of the strong affinity between the carboxylate groups of the CNDs and surface Ti, C-O-Ti bonds[23] are formed as disclosed by XPS.

XRD is used to characterize the crystal phases as shown in Fig. 3(a). Before the thermal treatment, the nanotubes are amorphous. After annealing at 450 °C for 2 h, three peaks at $2\theta = 25.2°$, 37.8°, and 48.1° indexed to the crystalline phase of anatase TiO_2 (JCPDS No. 78-2486) emerge. After doping of the CNDs, the intensity of the diffraction peaks of anatase diminishes slightly possibly due to the XRD imaging geometry. Raman scattering confirms the existence of CNDs as shown in Fig. 3(b). The Raman spectrum of TiNTs exhibits three peaks at 398 cm^{-1}, 515 cm^{-1}, and 636 cm^{-1}, which can be assigned to the B_{1g}, $A_{1g}+B_{1g}$, and E_g modes of anatase TiO_2.[24] After decoration with CNDs, two additional peaks at 1588 cm^{-1} and 1365 cm^{-1} appear. The former peak is the G band of carbon, and the latter is the D band caused by the disorderly network of sp^2 and sp^3 carbon clusters. The D band to G band intensity ratio is about 0.76, suggesting the presence of π-π conjugation at the sp^2 sites of the CNDs.[25] There is no noticeable peak shift or new peak in the range between 200 and 800 cm^{-1} [Fig. 3(b)].

The XPS patterns confirm the formation of CNDs/TiNTs. As shown in Fig. 4(a), the XPS survey spectrum of

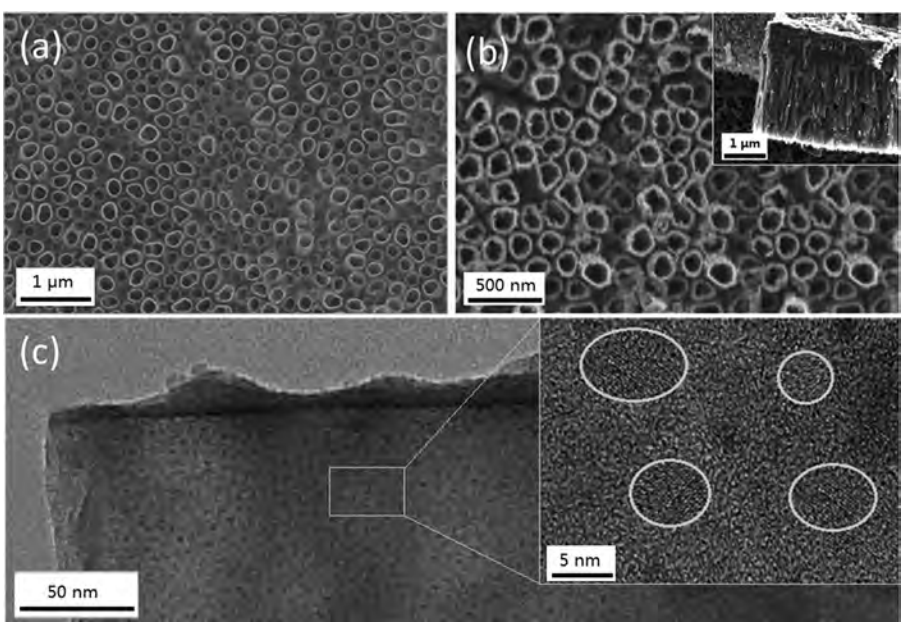

FIG. 2. (a) SEM image of the as-produced anatase TiNTs. (b) SEM image of the as-synthesized CNDs/TiNTs with the inset showing the lateral image of the nanotubes. (c) TEM and HR-TEM (inset) images of the CNDs/TiNTs. The white circle is the crystalline structure of the CNDs with an interplanar distance of 0.32 nm consistent with the lattice spacing of the (002) graphitic carbon.

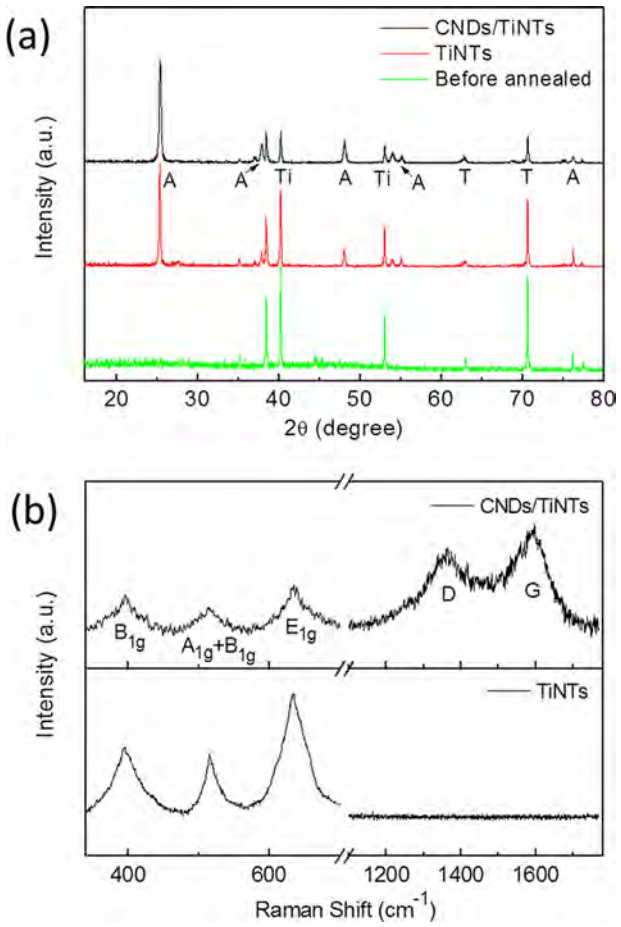

FIG. 3. (a) XRD patterns of CNDs/TiNTs and TiNTs after and before annealing; Label (A) represents the anatase phase of TiO_2 and (T) is titanium. (b) Raman scattering spectra of TiNTs and as-prepared CNDs/TiNTs.

CNDs/TiNTs shows the presence of Ti, O, and C. In comparison with TiNTs, the relative intensity of the C peak in CNDs/TiNTs is larger, meaning there is more C on the surface. Figure 4(b) shows the Ti 2p core level XPS spectrum, and the two peaks at 458.6 eV and 464.3 eV are Ti $2p_{3/2}$ and Ti $2p_{1/2}$ for Ti (IV) of titania, respectively. There is no obvious difference between the two samples indicating that the carbon atoms are scarcely incorporated into the TiO_2 lattice. The C 1s spectrum in Fig. 4(c) shows peaks at 284.6 eV, 285.6 eV, and 288.5 eV peaks arising from elemental carbon, C-O, and C=O, respectively. As shown in Fig. 4(d), the peaks at 529.8 and 531.4 eV are attributed to surface oxygen complexes of TiO_2 and carbon phases. The surface oxygen complexes of the carbon phase support the strong interphase structural effect between carbon and metal oxide in the Ti-O-C structure.[23] The oxygen and titanium concentrations in CNDs/TiNTs are 38.10% and 11.60%, respectively, and the O/Ti atomic ratio is about 3.3 that is above the stoichiometric value of TiO_2. In comparison, the oxygen and titanium concentrations in TiNTs are 46.01% and 19.05%, respectively, and the larger oxygen concentration in CNDs/TiNTs stems from CNDs.

The photocatalytic experiments are performed on a home-made device. The vessel is immersed in a sink in which water is kept at about 20 °C. The photocatalytic activity is evaluated by photocatalytic degradation of methylene blue (MB) with a 400 W Xe lamp as the irradiation source. The TiO_2 samples (3.0 cm × 2.0 cm) were immersed in 20 ml of MB (3 mg/l) and stirred for 1 h to reach adsorption equilibrium before irradiation. The concentration of MB was determined at intervals of 20 min by UV-Vis spectrophotometry in the wavelength range between 400 and 800 nm. A 600 nm short-pass (SP) filter and a 600 nm long-pass (LP) filters were employed to select the wavelength ranges. The 600 nm LP filter is used to remove light with wavelengths below 600 nm (Condition-1), and the 600 nm SP filter allows light with wavelengths shorter than 600 nm to pass (Condition-2).

Each photo-degradation experiment was repeated three times, and the average results are presented in Fig. 5. In Fig. 5(a), curve 1 indicates that degradation of CNDs/TiNTs is

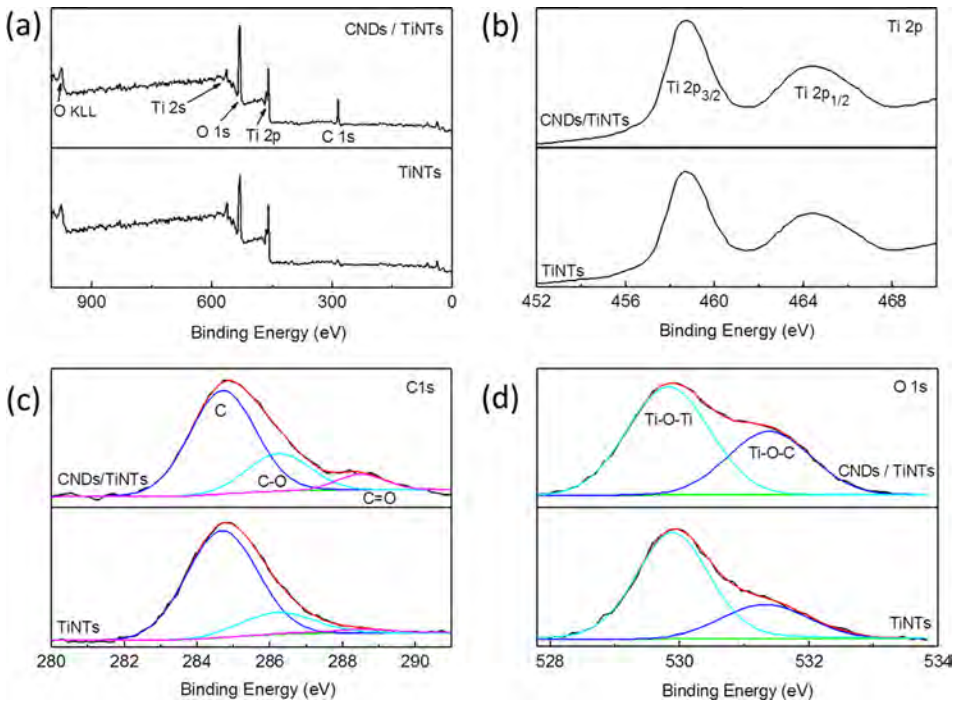

FIG. 4. XPS spectra of CNDs/TiNTs and TiNTs: (a) Survey spectra; (b) Ti 2p; (c) C 1s; and (d) O 1s.

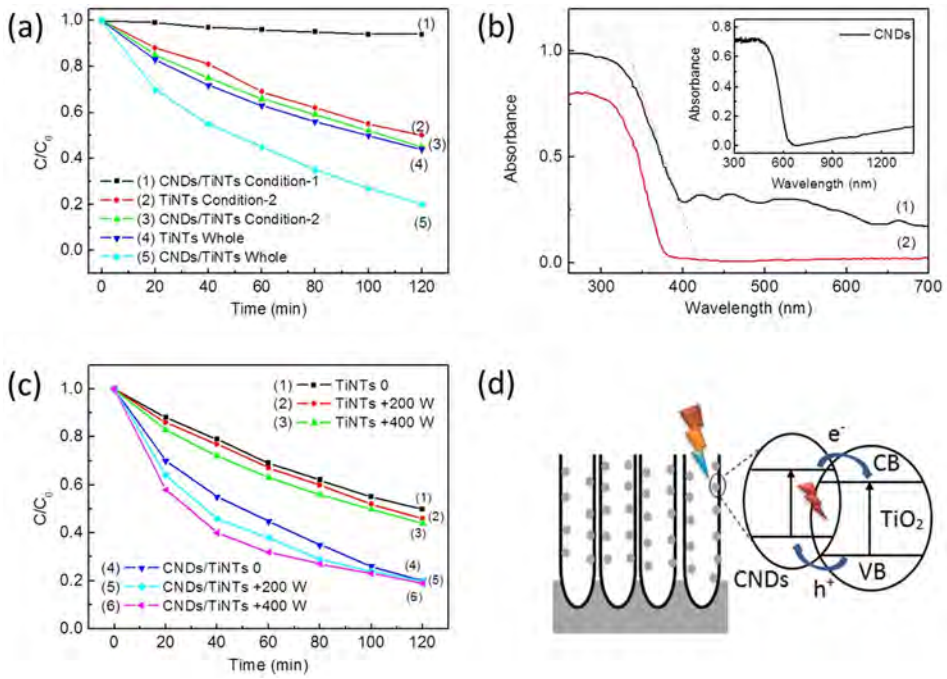

FIG. 5. (a) Photocatalytic degradation of MB on TiNTs or CNDs/TiNTs; (b) UV-Vis diffuse reflectance absorption spectra of CNDs/TiNTs (curve 1) and TiNTs (curve 2) with the inset showing the UV-Vis diffuse reflectance absorption spectra of CNDs. (c) Photocatalytic degradation of MB on TiNTs or CNDs/TiNTs illuminated with two lamps. Lamp 1 with a fixed power provides light throughout the entire wavelength range, and lamp 2 delivers variable power (above 600 nm) (inset) (d) Schematic illustration of organic pollutant degradation under Xe light irradiation.

negligible under Condition-1, indicating that there are almost no chemically active electrons generated by light above 600 nm. Curves 2 and 3 show MB degradation by TiNTs and CNDs/TiNTs under Condition-2, respectively, and curves 4 and 5 correspond to TiNTs and CNDs/TiNTs illuminated with the xenon lamp without a filter (that is, light covering the entire wavelength range) and the condition is labeled as whole. By comparison of curves 2 and 3, 4 and 5, CNDs/TiNTs shows higher catalytic activity. The degradation rate is reduced somewhat when the SP filter is used because the filter partially attenuates visible light.

The enhancement in the photocatalytic property can be explained by larger light absorption which plays a key role in the utilization of solar energy. The UV-Vis diffuse reflectance absorption spectra of TiNTs and CNDs/TiNTs are displayed in Fig. 5(b). The bandgap of TiNTs is calculated to be 3.2 eV, which is consistent with anatase TiO_2 revealed by XRD, and the bandgap of CNDs/TiNTs is 2.97 eV according to the measurement. The red-shift of the absorption edge extends absorption, thus enhancing photocatalytic characteristics.[26] In addition, the gap between curves 3 and 5 is larger than that between curves 2 and 4. This phenomenon is attributed to the thermal effect of CNDs/TiNTs. As shown in the inset in Fig. 5(b), the CNDs exhibit optical absorption in the infrared region, and so, the CNDs are promising in photothermal applications.[27,28]

There may be four reasons for the improved catalytic properties of the CNDs/TiNTs. First, the CNDs enhance absorption of organic molecules on the surface, and second, the CNDs adhered onto the TiNTs can change the band structure as shown in Fig. 5(b). It can absorb more light and generate more electrons and holes. Third, the CNDs introduce a larger catalytic interface to inhibit recombination of electrons and holes. Under irradiation, the CNDs inject photo-induced electrons into the TiO_2 conduction band and trigger the formation of the reactive radicals, $OH^{\bullet}$ and $O_2^{\bullet}$. The fourth factor is the thermal effect. Two lamps are used to verify the thermal effect of CNDs/TiNTs as shown in Fig. 5(c). The xenon lamp with a 300 W fixed power and without a filter is placed on top and labeled as lamp 1. Lamp 2 placed besides lamp 1 produces light above 600 nm, and the power can be adjusted (200 W, 400 W) to study the impact of light irradiation. As shown in Fig. 5(c) (curves 1–3), degradation of MB by TiNTs is enhanced slightly in the presence of lamp 2, meaning that light over 600 nm has little effects on the photocatalytic characteristics. Curves 4–6 show improved photocatalytic performance of CNDs/TiNTs and light above 600 nm plays an important role in the photocatalytic performance of CNDs/TiNTs.

In the photo-degradation process, although the temperature of the vessel is kept constant, CNDs generate thermal energy which affects the transportation of photo-generated carriers. With regard to CNDs, the photo-induced carriers have a hot distribution, and the energy relaxation is dominated by carrier-phonon scattering. Owing to the small PL quantum yield of CNDs, a large amount of phonons are emitted from the excited spot. These phonons alter the phonon distribution on the surface of TiO_2 nanotubes and the local spot temperature is higher. Therefore, the carriers experience a higher site-specific lattice temperature which has a positive influence on catalysis. The possible mechanism for electron transfer[26,29] and photocatalytic degradation of MB is shown in Fig. 5(d). The detailed data illustrating that the CNDs increase the solution temperature are presented in Fig. S2 in supplementary material. It is unlikely that the upconversion photoluminescence (UCPL) of CNDs affects photocatalysis because UCPL occurs with coherent photons regardless of the underlying mechanism. In fact, under Xe lamp irradiation, it is difficult to get upconversion from CNDs.[30]

In summary, CNDs can extend the absorption edge of TiO_2 and enhance degradation of organic pollutants by TiNTs. Under xenon lamp illumination, irradiation not only induces electrons and holes, but also can heats the CNDs-TiO_2 at local spots because of the photothermal effect. This

causes electrons to obtain more energy, thereby promoting degradation of pollutants by the nanocomposites. Similar effects are believed to occur on other CNDs-based nanocomposites and are important to photocatalysis. CNDs based nanocomposites with improved photothermal performance are promising in photocatalysis pertaining to environment and energy applications.

See supplementary material for the degradation activity of the samples synthesized with different concentrations of CNDs and the photothermal effect of CNDs.

The work was supported by City University of Hong Kong Applied Research, Grants (ARG) Nos. 9667122 and 9667144, as well as Natural Science Foundation of the Higher Education Institutions of Education Department of Jiangsu Province, Grant No. 16KJB430004.

[1]Y. M. Kang, C. W. Wang, J. B. Chen, L. Q. Wang, D. S. Li, W. D. Zhu, and F. Zhou, J. Vac. Sci. Technol. B **30**(4), 041801 (2012).
[2]M. Z. Ge, C. Y. Cao, J. Y. Huang, S. H. Li, S. N. Zhang, S. Deng, Q. S. Li, K. Q. Zhang, and Y. K. Lai, Nanotechnol. Rev. **5**(1), 75–112 (2017).
[3]Z. Lan, W. X. Wu, S. Zhang, L. F. Que, and J. H. Wu, J. Solid State Electrochem. **20**, 2643–2650 (2016).
[4]P. Gorbovyi, A. Uklein, S. Tieng, O. Brinza, M. Traore, K. Chhor, L. Museur, and A. Kanaev, Nanoscale **3**, 1807–1812 (2011).
[5]H. Y. Wang, G. M. Wang, Y. C. Ling, M. Lepert, C. C. Wang, J. Z. Zhang, and Y. Li, Nanoscale **4**, 1463–1466 (2012).
[6]B. Mukherjee, W. Wilson, and V. Subramanian, Nanoscale **5**, 269–274 (2013).
[7]X. M. Li, M. C. Rui, J. Z. Song, Z. H. Shen, and H. B. Zeng, Adv. Funct. Mater. **25**, 4929–4947 (2015).
[8]K. Hola, Y. Zhang, Y. Wang, E. P. Giannelis, R. Zboril, and A. L. Rogachb, Nano Today **9**, 590–603 (2014).
[9]M. Zheng, S. Liu, J. Li, D. Qu, H. F. Zhao, X. A. Guan, X. L. Hu, Z. A. Xie, X. B. Jing, and Z. C. Sun, Adv. Mater. **26**, 3554–3560 (2014).
[10]R. Miao, Z. Luo, W. Zhong, S. Y. Chen, T. Jiang, B. Dutta, Y. Nasr, Y. S. Zhang, and S. L. Suib, Appl. Catal. B Environ. **189**, 26–38 (2016).
[11]J. Liu, Y. Liu, N. Y. Liu, Y. Z. Han, X. Zhang, H. Huang, Y. Lifshitz, S. T. Lee, J. Zhong, and Z. H. Kang, Science **347**, 970–974 (2015).
[12]P. Mirtchev, E. J. Henderson, N. Soheilnia, C. M. Yip, and G. A. Ozin, J. Mater. Chem. **22**, 1265–1269 (2012).
[13]H. Zhang, H. Ming, S. Lian, H. Huang, H. Li, L. Zhang, Y. Liu, Z. Kang, and S.-T. Lee, Dalton Trans. **40**, 10822–10825 (2011).
[14]H. T. Li, X. D. He, Z. H. Kang, H. Huang, Y. Liu, J. L. Liu, S. Y. Lian, C. H. A. Tsang, X. B. Yang, and S. T. Lee, Angew. Chem., Int. Ed. **49**, 4430–4434 (2010).
[15]Q. Lou, S. N. Qu, P. T. Jing, W. Y. Ji, D. Li, J. S. Cao, H. Zhang, L. Liu, J. L. Zhao, and D. Z. Shen, Adv. Mater. **27**, 1389–1394 (2015).
[16]T. Qin, Z. Y. You, H. Wang, Q. H. Shen, F. Zhang, and H. Yang, J. Electrochem. Soc. **164**(4), H211–H214 (2017).
[17]Z. J. Zhang, T. T. Zheng, X. M. Li, J. Y. Xu, and H. B. Zeng, Part. Part. Syst. Charact. **33**, 457–472 (2016).
[18]J. Zhang, Y. Ma, Y. L. Du, H. Z. Jiang, D. D. Zhou, and S. S. Dong, Appl. Catal., B **209**, 253–264 (2017).
[19]J. C. Ge, Q. Y. Jia, W. M. Liu, L. Guo, Q. Y. Liu, M. H. Lan, H. Y. Zhang, X. M. Meng, and P. F. Wang, Adv. Mater. **27**, 4169–4177 (2015).
[20]J. Zhang, L. Z. Liu, L. Yang, Z. X. Gan, X. L. Wu, and P. K. Chu, Appl. Phys. Lett. **104**, 231902 (2014).
[21]J. Tang, Y. Y. Zhang, B. Kong, Y. C. Wang, P. M. Da, J. Li, A. A. Elzatahry, D. Y. Zhao, X. G. Gong, and G. F. Zheng, Nano Lett. **14**, 2702–2708 (2014).
[22]O. E. Semonin, J. C. Johnson, J. M. Luther, A. G. Midgett, A. J. Nozik, and M. C. Beard, J. Phys. Chem. Lett. **1**, 2445 (2010).
[23]Y. Huang, W. K. Ho, S. C. Lee, L. Z. Zhang, G. S. Li, and J. C. Yu, Langmuir **24**, 3510–3516 (2008).
[24]H. Wang, X. Quan, H. T. Yu, and S. Chen, Carbon **46**, 1126–1132 (2008).
[25]W. Y. Rho, H. S. Kim, H. M. Kim, J. S. Suh, and B. H. Jun, New J. Chem. **41**, 285–289 (2017).
[26]M. Y. Sun, S. N. Qu, W. Y. Ji, P. T. Jing, D. Li, L. Qin, J. S. Cao, H. Zhang, J. L. Zhao, and D. Z. Shen, Phys. Chem. Chem. Phys. **17**, 7966–7971 (2015).
[27]M. X. Sun, X. Q. Ma, X. Chen, Y. J. Sun, X. L. Cui, and Y. H. Lin, RSC Adv. **4**, 1120 (2014).
[28]D. Li, D. Han, S. N. Qu, L. Liu, P. T. Jing, D. Zhou, W. Y. Ji, X. Y. Wang, T. F. Zhang, and D. Z. Shen, Light: Sci. Appl. **5**, e16120 (2016).
[29]G. B. Markad, S. Kapoor, S. K. Haram, and P. Thakur, Sol. Energy **144**, 127–133 (2017).
[30]Z. X. Gan, X. L. Wu, G. X. Zhou, J. C. Shen, and P. K. Chu, Adv. Opt. Mater. **1**, 554–558 (2013).

Supplementary Materials

Carbon Nanodots-Based Nanocomposites with enhanced photocatalytic performance and Photothermal effects

J. Zhang[1*], Y. L. Tang[1], G. Hu, B. L. Gao,[1] Z. X. Gan,[3] and Paul K. Chu[2*]

[1] Faculty of Mathematics and Physics, Huaiyin Institute of Technology, Huaian 223003, China

[2] Department of Physics and Materials Science, City University of Hong Kong, Tat Chee Avenue, Kowloon, Hong Kong, China

[3] School of Physics and Technology, Nanjing Normal University, Nanjing 210023, China

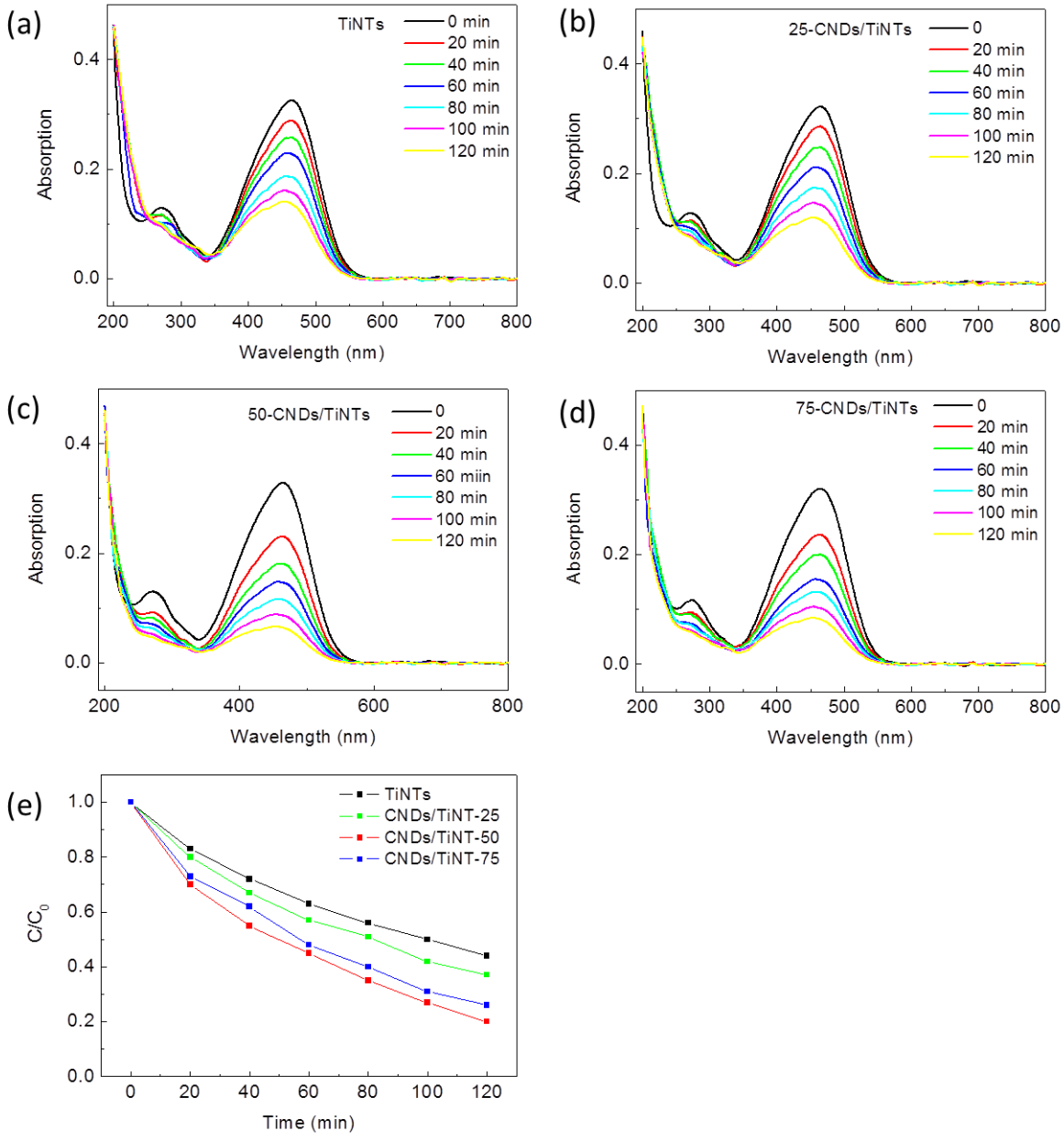

Fig S1. (a-d) UV-Vis absorption spectra of different samples after decolorization of methyl blue; (e) Comparison of the catalyst activity.

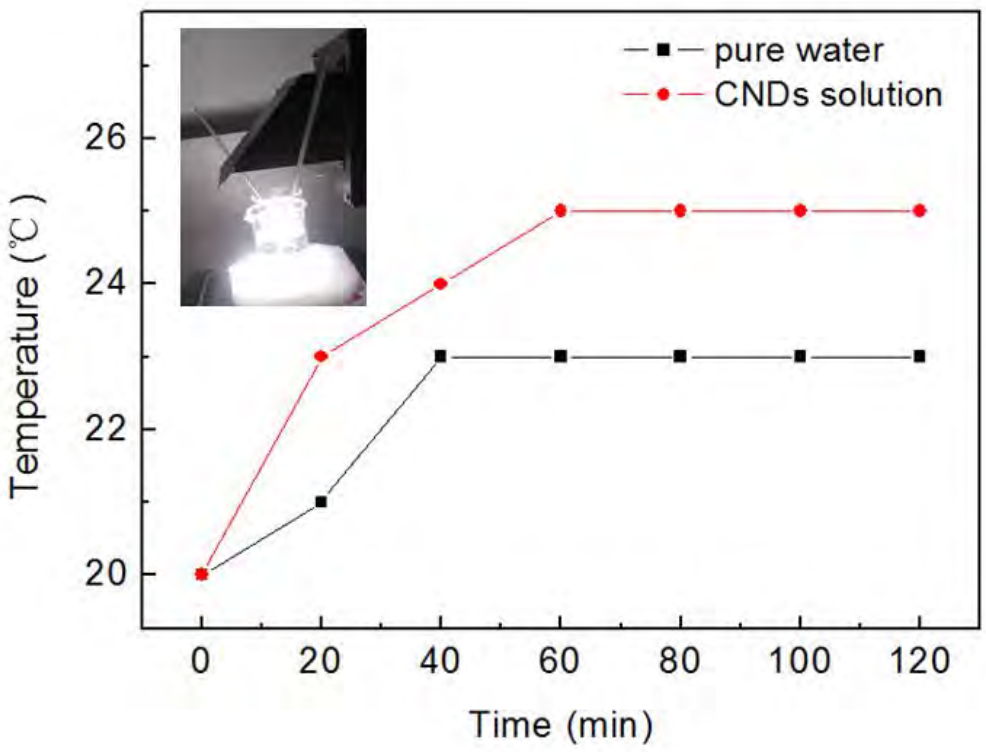

Fig. S2. A beaker with 200 ml (5 μg/ml) of the CNDs solution and another beaker containing deionized water were placed under thje Xe light (300W) and the temperature was measured by two household thermometers with a precision of 0.1℃. After 40 minutes, the DI water reached equilibrium and a temperature of 23℃, whereas the CNDs solution reached equilibrium after 60 min and a temperature of 25℃. The inset shows the photograph of the experimental setup.